A New Formulation of Pocklington's Equation for Thin Wires Using the Exact Kernel

Ebrahim Forati, Aaron D. Mueller, Parisa Gandomkar Yarandi, and George W. Hanson

***Abstract*—Pocklington's integro-differential equation for thin wires with the exact kernel is reformulated using a second derivative formula for improper integrals. This allows for analytical evaluation of the second derivatives, resulting in a pure integral equation, in a similar manner to what is done when using the approximate kernel. However, as opposed to using the approximate kernel, the resulting integral equation developed here is numerically stable even with a simple pulse function/point matching solution. Good convergence for the current is obtained using pulse functions, and the severe unphysical oscillations of the current that are encountered when using pulse functions with the approximate kernel are avoided.**

***Index Terms*—Electromagnetic theory, integral equations.**

I. Introduction

Pocklington's integro-differential equation is a staple of thin-wire antenna analysis, and appears in most antenna text books [1]–[4], as well as forming the basis of antenna simulation codes such as the Numerical Electromagnetics Code (NEC) [5]. As typically presented, for a wire of length $2L$ centered and oriented along the z axis, Pocklington's equation is

$$\frac{1}{4\pi j\,\omega\varepsilon}\left(k^2+\frac{\partial^2}{\partial z^2}\right)\int_{-L}^{L} K(z-z')I(z')dz' = E_z^i(z) \qquad (1)$$

for $-L \le z \le L$, where $I(z)$ is the wire current (A), $k^2=\omega^2\mu\epsilon$ with μ,ε characterizing the homogeneous space outside of the wire, E_z^i is the incident field, and

$$K(z-z') = \frac{1}{2\pi}\int_{-\pi}^{\pi}\frac{e^{-jkR}}{R}d\phi' = \frac{1}{2\pi}\int_{-\pi}^{\pi}\frac{e^{-jk\sqrt{(z-z')^2+4a^2sin^2(\phi'/2)}}}{\sqrt{(z-z')^2+4a^2sin^2(\phi'/2)}}d\phi' \qquad (2)$$

is the so-called exact kernel. This equation applies to a perfectly-conducting wire of radius a that is electrically thin (i.e., $a \ll \lambda$, where λ is the free-space wavelength). Because of the perfect electrical conductor (PEC) approximation, all current resides on the wire surface, and due to the electrical thinness assumption, small radial and circumferential currents have been ignored, as has the circumferential variation of the axial current.

Manuscript received November 27, 2010; revised April 01, 2011; accepted June 02, 2011. Date of publication August 12, 2011; date of current version November 02, 2011.

The authors are with the Department of Electrical Engineering, University of Wisconsin-Milwaukee, Milwaukee, WI 53211 USA (e-mail: george@uwm.edu).

Color versions of one or more of the figures in this communication are available online at http://ieeexplore.ieee.org.

Digital Object Identifier 10.1109/TAP.2011.2164211

Pocklington's equation (1) is somewhat difficult to work with since the second derivative cannot be simply brought inside the integral (the resulting integral over z' is non-convergent). For this reason, (1) is often converted to Hallén's equation [4] for numerical solution. Alternatively, it is common to work with Pocklington's equation directly and make the approximation [4]

$$K(z-z') \simeq K_a(z-z') = \frac{e^{-jk\sqrt{(z-z')^2+a^2}}}{\sqrt{(z-z')^2+a^2}} \qquad (3)$$

where $K_a(z-z')$ is known as the approximate kernel. Using the approximate kernel, the second derivatives can be brought inside the integral and $\partial^2 K_a(z-z')/\partial z^2$ can be evaluated explicitly, resulting in a simple formulation involving proper integrals that are easy to program.

However, there are both theoretical and numerical problems associated with the approximate kernel. Theoretically, Pocklington's equation with the approximate kernel has no solution [6]–[9], whereas Pocklington's equation with the exact kernel is well-posed, at least in suitable function spaces [7], [10]–[12]. Despite this important fact, Pocklington's equation with the approximate kernel often yields numerical results that agree fairly well with results obtained using the exact kernel. However, a numerical problem arises when using sub-domain functions for the current expansion, such as pulse functions

$$I(z) = \sum_{n=1}^{N} a_n f_n(z) \qquad (4)$$

where

$$f_n(z) = \begin{cases} 1 & z_n - \frac{\Delta}{2} < z \le z_n + \frac{\Delta}{2} \\ 0 & \text{otherwise} \end{cases}$$

are the usual pulse functions and a_n's are the unknown coefficients to be determined, and where $\Delta = 2L/N$, and $z_n = -L+(n-1/2)\Delta$. A well-known problem of the approximate kernel is that one must ensure $\Delta/a > 1$ [9], otherwise severe and non-physical oscillations in the current appear in the numerical solution (although this is often not mentioned in elementary textbooks). Thus, a value of N must be chosen that is large enough to yield a "good" result but small enough so that the condition $\Delta/a > 1$ is not violated. This is a rather unsatisfactory solution, and a similar problem exists even for entire-domain basis functions [13]. It is possible to use the exact kernel and bring one derivative inside the integral, integrate by parts to move the derivative onto the current, and then bring the second derivative inside the integral. However, in solving the resulting equation one needs to use suitably smooth expansion functions, and a pulse-function solution is not possible.

In this work, we show that the use of a rigorous method (similar to a Leibnitz rule [14]) for interchanging the second derivative and integral in (1) leads to a purely integral formulation of Pocklington's equation with the exact kernel that is simple and easy to program. Even for pulse functions, stable results are obtained with no restriction on the ratio Δ/a.

Other papers, such as [15]–[21] also discuss rigorous methods involving the exact kernel, and utilize either expansions of the kernel, efficient methods of treating the singularity, the use of suitable basis functions, or some combination of these techniques. A comparison among the various methods is beyond the scope of this work, although it can be noted that the method presented here is straightforward in concept and simple to implement.

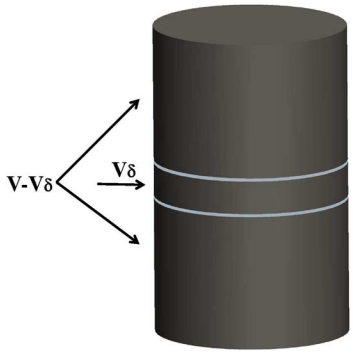

Fig. 1. Solid wire geometry showing exclusion volume V_δ.

II. Theory and Formulation

The starting point for the Pocklington equation derivation is the relationship between current density and electric field, which, in a homogeneous medium, is [22]–[24]

$$\mathbf{E}^s(\mathbf{r}) = \frac{1}{j\omega\varepsilon}\left(k^2 + \nabla\nabla\bullet\right) lim_{\delta\to 0} \int\limits_{V-V_\delta(\mathbf{r})} g(\mathbf{r},\mathbf{r}')\mathbf{J}(\mathbf{r}')dV' \tag{5}$$

where $V_\delta(\mathbf{r})$ is an exclusion volume [22] as depicted in Fig. 1 (when $\mathbf{r}$ is not in the source region the limiting procedure is not necessary)

$$g(\mathbf{r},\mathbf{r}') = \frac{e^{-jk|\mathbf{r}-\mathbf{r}'|}}{4\pi|\mathbf{r}-\mathbf{r}'|} = \frac{e^{-jkR}}{4\pi R}. \tag{6}$$

is the free-space Green's function, and $R = (\rho^2 + \rho'^2 - 2\rho\rho'\cos(\phi-\phi') + (z-z')^2)^{1/2}$. Assuming an electrically thin wire oriented along the z-axis, the small radial and circumferential currents and the circumferential variation of the axial current can be ignored, such that $\mathbf{J}(\rho,\varphi,z) \simeq \hat{\mathbf{z}}J_z(\rho,z)$.

In the following sections two different cases for thin wires are considered, a solid wire model and an infinitesimally-thin shell (hollow tube) model. For the PEC case the solid wire model is not needed, but it is included here since a) for generality we consider the more realistic imperfect conductor case, and b) it utilizes a known rigorous method to pass the second derivatives through the principle-value type volume integral in (5) (this is related to the well-known depolarizing dyadic problem [22]). For the hollow tube model we present a new two-dimensional second-derivative formula for this interchange of operators. Both the solid wire and hollow tube cases result in the same expression, which is then used to form Pocklington's equation.

A. Case 1: Thin Solid Wire Model

In order to pass the second derivative through the volume integral we use the second derivative formula [24, see (1.59)], [25, p. 248; in this reference the static case is treated],

$$\begin{aligned}\frac{\partial^2}{\partial x_i \partial x_j} lim_{\delta\to 0} \int\limits_{V-V_\delta(\mathbf{r})} s(\mathbf{r}')g(\mathbf{r},\mathbf{r}')dV' \\ = -s(\mathbf{r}) \oint\limits_S \frac{\partial g(\mathbf{r},\mathbf{r}')}{\partial x_j}\hat{\mathbf{x}}_i \bullet \mathbf{n}dS' \\ + lim_{\delta\to 0} \int\limits_{V-V_\delta(\mathbf{r})} \left[s(\mathbf{r}') - s(\mathbf{r})\right] \frac{\partial^2 g(\mathbf{r},\mathbf{r}')}{\partial x_i \partial x_j} dV'.\end{aligned} \tag{7}$$

If the wire is thin ($a \ll \delta$, where δ is the skin depth), one can ignore the radial variation of the axial current, so that $J_z(\rho,z) \simeq I(z)/\pi a^2$. Moreover, since $g(\mathbf{r},\mathbf{r}')$ varies little over the radius of the wire (the singularity is excluded by isolation in the z-direction as depicted in Fig. 1) we can set $\rho = \rho' = a$ and $\phi = 0$ in R. Using (7), the z-component of (5) can be written as

$$E_z^s(\mathbf{r}) = I_1 + I_2 + I_3 \tag{8}$$

where

$$I_1 = \frac{k^2}{4\pi j\omega\varepsilon}\mathrm{PV}\int\limits_{-L}^{L} K(z-z')I(z')dz', \tag{9}$$

$$\begin{aligned}I_2 &= -\frac{I(z)}{4\pi j\omega\varepsilon}\frac{\partial}{\partial z}\left[K(z-L) - K(z+L)\right], \quad z \neq \pm L \\ &= 0, z = \pm L\end{aligned} \tag{10}$$

$$I_3 = \frac{1}{4\pi j\omega\varepsilon}\mathrm{PV}\int\limits_{-L}^{L}\left[I(z') - I(z)\right]\frac{\partial^2 K(z-z')}{\partial z^2}dz'. \tag{11}$$

The term I_1 simply comes from the k^2 term in (5). The second two terms arise from (7). Note that I_2, which comes from the first term on the right side of (7), is zero for $z = \pm L$. To explain this, consider that in (7), S is the surface of $V - V_\delta(\mathbf{r})$. This consists of the cylindrical surface (which doesn't contribute because of the unit vector $\hat{\mathbf{x}}_i = \hat{\mathbf{z}}$), the two end-caps, and two end-cap-like surfaces on the top and bottom of $V_\delta(\mathbf{r})$. These latter two contributions cancel each other and give zero contribution. That leaves the two actual end-caps. However, e.g., if $z = L$ then $V_\delta(\mathbf{r})$ is centered on $z = L$ and so there is no end-cap contribution from that point, which would otherwise contribute the $K(z-L)$ term. In this case the only contribution from S is the other end cap, which contributes the non-singular term $K(z+L) = K(2L)$ term in I_2. Since $I(L) = 0$ then (10) gives no contribution. It follows that (10) contributes for all $z \neq \pm L$.

In both (9) and (11) the notation PV indicates the usual principle-value type integral that omits the singular point $z' = z$. Note that in (11) we cannot break up the integral into two integrals, since for this to be a valid operation the resulting two integrals must be convergent, which is not the case.

B. Case 2: Hollow Tube Model

This model is probably more familiar for thin-wire antenna analysis. In this case we assume that the wire is electrically thin ($a \ll \lambda$) yet thick compared to a skin depth ($a \gg \delta$), so that we can model the wire as an infinitesimally-thin hollow shell. Then, the z-component of (5) simplifies to

$$E_z^s(a,0,z) = \frac{1}{j\omega\varepsilon}\left(k^2 + \frac{\partial^2}{\partial z^2}\right) lim_{\delta\to 0} \int\limits_{s-s_\delta(\mathbf{r})} g(\mathbf{r},\mathbf{r}')\frac{I(z')}{2\pi a}dS' \tag{12}$$

where S is the open surface of the hollow tube (with rim C) and S_δ is an exclusion surface (with rim C_δ), as shown in Fig. 2.

In the Appendix, a new second derivative formula (30) is derived that is the two-dimensional, open-surface analogue of (7). Using this, we can write (12) as $E_z^s(z) = I_1 + I_2 + I_3$, where

$$I_1 = \frac{k^2}{j\omega\varepsilon} lim_{\delta\to 0} \int\limits_{s-s_\delta(\mathbf{r})} g(a,0,z,a,\varphi',z')\frac{I(z')}{2\pi a}ad\varphi'dz', \tag{13}$$

$$I_2 = -\frac{I(z)}{2\pi j\omega\varepsilon a}\oint\limits_C \mathbf{n}\bullet\hat{\mathbf{z}}\frac{\partial}{\partial z}g(a,0,z,a,\varphi',z')ad\varphi', \tag{14}$$

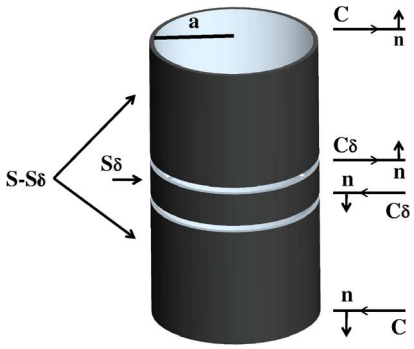

Fig. 2. Hollow tube geometry showing exclusion surface, S_δ. The rim C of the surface $S - S_\delta$, and the rim C_δ of exclusion surface S_δ, are depicted by the lines on the right side.

$$I_3 = \frac{1}{j\omega\varepsilon}\lim_{\delta\to 0}\int\limits_{s-s_\delta(\mathbf{r})}\left(\frac{I(z')}{2\pi a}-\frac{I(z)}{2\pi a}\right)\times\frac{\partial^2}{\partial z^2}g(a,0,z,a,\varphi',z')ad\varphi' dz'. \quad (15)$$

In (14), C is the boundary of the open surface S (i.e., the top and bottom rims shown in Fig. 1), which are not related to the open exclusion surface S_δ). One can easily show that (13)–(15) are the same as (9)–(11). As a result, the same equation for $E_z^s(z)$ is obtained for both cases.

C. Pocklington's Integral Equation

To form Pocklington's integral equation, for generality we will assume an imperfectly-conducting wire and use an impedance boundary condition, so that at the surface of the wire

$$E_z^{total}(z) = E_z^s(z) + E_z^i(z) = I(z)z_s \quad (16)$$

where z_s is the surface impedance (Ω/m) of the thin wire. Writing $E_z^s = I_1 + I_2 + I_3$ we have, for $-L < z < L$,

$$\begin{aligned} k^2\mathrm{PV}\int_{-L}^{L}K(z-z')I(z')dz' - I(z)\frac{\partial}{\partial z}&\times[K(z-L)-K(z+L)]\\ &+\mathrm{PV}\int_{-L}^{L}\left[I(z')-I(z)\right]\frac{\partial^2 K(z-z')}{\partial z^2}dz'\\ &= 4\pi j\omega\varepsilon\left(I(z)z_s - E_z^i(z)\right). \end{aligned} \quad (17)$$

This is the main result of the communication. This integral equation is general, and can be solved using any suitable basis functions. Here we use pulse functions since they are simple, and provide an example where their use in the approximate/reduced kernel equation leads to poor results.

Note that for (17) we specify $-L < z < L$ rather than $-L \le z \le L$; for the second term on the left side (I_2) this ensures that the point $z = \pm L$ is excluded (see (10)). This term is easy to evaluate numerically since it does not involve integration. The first term on the left side (I_1) is easy to evaluate numerically, being an undifferentiated potential (the PV notation is somewhat superfluous, and simply indicates that the integral is improper (yet convergent)). The third term on the left side (I_3) is also easy to evaluate numerically due to the current difference$I(z') - I(z)$. In particular, in a pulse function point matching solution (matching points z_m, $m = 1, 2, \ldots N$) the third term is

$$\begin{aligned} I_3 &= \int_{-L}^{L}\left[\sum_{n=1}^{N}a_n f_n(z') - a_m\right]\frac{\partial^2}{\partial z^2}K(z-z')_{z=z_m}dz'\\ &= \sum_{\substack{n=1\\ n\neq m}}^{N}(a_n - a_m)\int_{z_n-\triangle/2}^{z_n+\triangle/2}\frac{\partial^2}{\partial z^2}K(z-z')_{z=z_m}dz'. \end{aligned} \quad (18)$$

For the pulse function point matching solution, (17) becomes the matrix equation

$$[Z_{mn}]_{N\times N}[a_n]_{N\times 1} = [V_n]_{N\times 1} \quad (19)$$

where

$$\begin{aligned} Z_{mm} &= k^2\int_{z_m-\frac{\triangle}{2}}^{z_m+\frac{\triangle}{2}}K(z_m-z')dz'\\ &\quad-\sum_{\substack{n=1\\ n\neq m,\, z_n-\frac{\triangle}{2}}}^{N}\int^{z_n+\frac{\triangle}{2}}\frac{\partial^2}{\partial z^2}K(z-z')_{z=z_m}dz'\\ &\quad-\frac{\partial}{\partial z}\left[K(z-L)-K(z+L)\right]_{z=z_m} - j4\pi\omega\varepsilon z_s,\\ Z_{\substack{mn\\ m\neq n}} &= \int_{z_n-\frac{\triangle}{2}}^{z_n+\frac{\triangle}{2}}\left(k^2+\frac{\partial^2}{\partial z^2}\right)K(z-z')_{z=z_m}dz', \end{aligned} \quad (20)$$

and $V_m = -j4\pi\omega\varepsilon E_z^i(z_m)$.

TABLE I
COMPARISON OF $|I(0)|(\mu\mathrm{A})$ BETWEEN THE NEW POCKLINGTON FORM AND HALLÉN'S EQUATION WITH EXACT KERNEL FOR THE CASE CONSIDERED IN FIG. 3

N	Pocklington	Hallén	% Δ
100	40.0187	40.0390	0.365
300	40.0177	40.0117	0.150
500	40.0171	40.0134	0.092
1000	40.0167	40.0148	0.046
2000	40.0165	40.0155	0.024
3000	40.0164	40.0157	0.0157
4000	40.0163	40.0159	0.0118
5000	40.0163	40.0159	0.0094

III. RESULTS

In all results we assume that a unit-amplitude plane wave is normally-incident on the wire, $f = 10\ \mathrm{GHz}$, $a = 0.005\lambda$, and we vary L and N. In all plots $\sigma = 5.9\times 10^7\ \mathrm{S/m}$.

Fig. 3 shows the current for $L = \lambda/2$ and $N = 61$ ($\Delta/a = 3.28$), so that the approximate kernel is expected to perform reasonably well. As can be seen from the figure, the current determined by using the approximate kernel (3) in (1) and the current obtained from the new integral equation (17) agree very well.

The new integral equation (17) was also verified by comparing to Hallén's equation using the exact kernel, where excellent agreement was found. Table I shows the current at the center of the wire for the

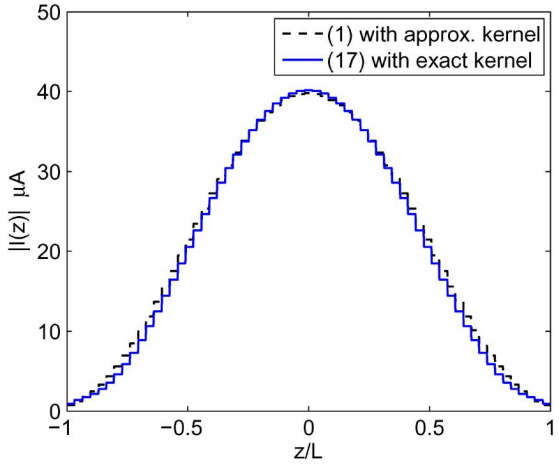

Fig. 3. Magnitude of the current obtained by using the approximate kernel in (1) and by the new integral equation (17) for $L = \lambda/2$ and $N = 61$. Since $\Delta/a > 1$ the approximate kernel is expected to yield good results.

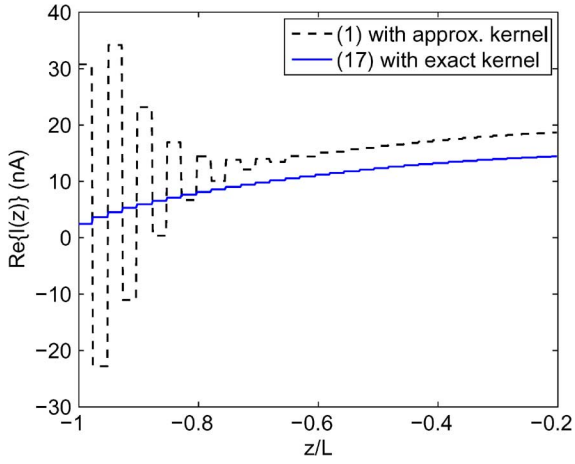

Fig. 4. Real part of the current for $L = \lambda/20$ and $N = 81$, where $\Delta/a = 0.25$, such that the approximate kernel is not expected to provide accurate results. The new integral equation (17) uses the exact kernel and avoids the problem of current oscillations near the wire ends arising from use of the approximate kernel.

geometry considered in Fig. 3. The last column is the percent difference between the two results. It can be seen that the Pocklington form converges faster than the Hallén form; for the Pocklington form the percent difference between the $N = 100$ and $N = 5000$ results is 0.06%, whereas for the Hallén form it is 0.3%.

Regarding computer times, both the new Pocklington form and the Hallén form only depend on $z - z'$, and thus have a Toeplitz form. Only the first row of the matrix need be filled, and thus both methods are very efficient. Computing the new Pocklington form takes approximately twice as long as the Hallén form since it involves numerical integration of two different integrands (K and $\partial^2 K/\partial z^2$), whereas the Hallén form involves only K. On a standard PC matrix fill time for either method is under a second for $N = 300$.

Fig. 4 shows the current for $L = \lambda/20$ and $N = 81$ ($\Delta/a = 0.25$), such that the approximate kernel is not expected to provide accurate results. Indeed, using the approximate kernel non-physical oscillations in the current appear at the wire ends, as discussed in [9] (for a delta-gap generator these oscillations occur near the wire center). However, the current obtained from (17) does not exhibit these non-physical oscillations, as we would expect when using the exact kernel.

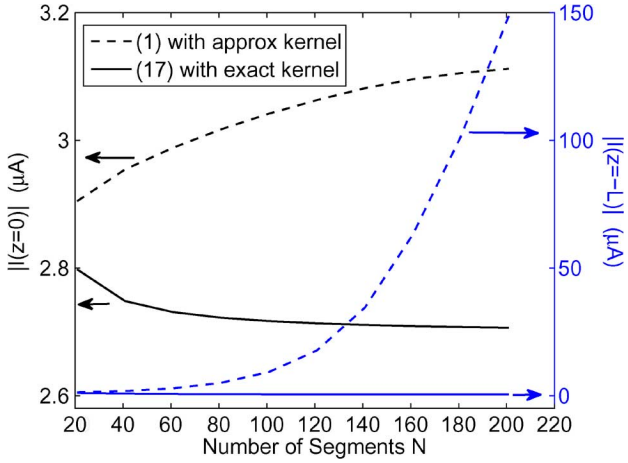

Fig. 5. Magnitude of the current at the wire center and at the wire ends obtained from the two methods for $L = \lambda/20$. The new formulation (17) yields results that converge very well at all points on the wire.

Fig. 5 shows a convergence study for the current at the wire center and near the wire ends obtained from the two methods, for $L = \lambda/20$. The approximate kernel yields a result that slowly converges to a value that is approximately 12% too large, and which diverges near the wire ends as N is increased, as expected. The new formulation (17) yields results that converge quickly at all points on the wire.

IV. Conclusions

Pocklington's integro-differential equation for thin wires with the exact kernel has been reformulated into a pure integral equation using a second derivative formula for improper integrals. Solid wire and hollow tube models have been considered. It was shown that a simple pulse-function point matching solution of the resulting integral equation leads to results that are stable and show good convergence, and which avoids the severe and non-physical oscillations of the current that arise from the same numerical procedure used in conjunction with the approximate kernel.

Appendix

To obtain the second derivative formula similar to (7) but for open surfaces, consider the quantity

$$\phi(\mathbf{r}) = \phi(a,\phi,z) = \lim_{\delta\to 0} \int_{S-S_\delta} s(\mathbf{r}')g(\mathbf{r},\mathbf{r}')dS' \tag{21}$$

where S is the surface of a hollow, infinitesimally-thin tube and S_δ is an exclusion surface, depicted in Fig. 2. The quantity (21) defines a single-layer potential with source density s. It is well-known that a tangential derivative of (21) can be passed through the integral (normal derivatives generate a term $\pm s(\phi,z)/2$, where (ϕ,z) is a point on the surface [26], [27]). Therefore,

$$\begin{aligned}\frac{\partial}{\partial z}\phi(\mathbf{r}) &= -\lim_{\delta\to 0}\int_{S-S_\delta} s(\mathbf{r}')\frac{\partial}{\partial z'}g(\mathbf{r},\mathbf{r}')dS' \\ &= \lim_{\delta\to 0}\left[\int_{S-S_\delta}\frac{\partial s(\mathbf{r}')}{\partial z'}g(\mathbf{r},\mathbf{r}')dS' \right. \\ &\qquad \left. -\int_{S-S_\delta}\nabla\bullet\left(\hat{\mathbf{z}}s(\mathbf{r}')g(\mathbf{r},\mathbf{r}')\right)dS'\right]\end{aligned}$$

$$= \lim_{\delta \to 0} \left[- \oint_{C+C_\delta} \mathbf{n} \bullet \hat{\mathbf{z}} s(\mathbf{r}') g(\mathbf{r}, \mathbf{r}') dl' + \int_{S-S_\delta} \frac{\partial s(\mathbf{r}')}{\partial z'} g(\mathbf{r}, \mathbf{r}') dS' \right] \quad (22)$$

where we use $\partial g(\mathbf{r}, \mathbf{r}')/\partial z = -\partial g(\mathbf{r}, \mathbf{r}')/\partial z'$ in the first line and the product rule for derivatives to obtain the second line, and where the third line comes from the divergence theorem in two dimensions,

$$\int_S \nabla \bullet \mathbf{A} dS = \oint_C \mathbf{n} \bullet \mathbf{A} dl \quad (23)$$

where C is the contour of the open surface S. The two-dimensional divergence theorem is usually applied to open surfaces in the plane. However, it is valid for any compact differential manifold that is equipped with an inner product at each point; the inner product at a point on a tube in R^3 is simply the dot product on R^3 restricted to vectors tangent to the tube at the given point. In this case, these will be unit vectors parallel to the axis of the tube pointing away from the tube at the tube rims, i.e., $\mathbf{n} = \pm \hat{\mathbf{z}}$.

It can be easily shown that

$$\lim_{\delta \to 0} \oint_{C_\delta} s(\mathbf{r}') g(\mathbf{r}, \mathbf{r}') \hat{\mathbf{z}} \bullet \mathbf{n} dl' = 0 \quad (24)$$

where it should be noted that C_δ comprises both the top and bottom rims of S_δ, which are taken in opposing directions. Therefore, (22) converts to

$$\frac{\partial}{\partial z} \phi(\mathbf{r}) = - \oint_C \mathbf{n} \bullet \hat{\mathbf{z}} s(\mathbf{r}') g(\mathbf{r}, \mathbf{r}') dl' + \lim_{\delta \to 0} \left[\int_{S-S_\delta} \frac{\partial s(\mathbf{r}')}{\partial z'} g(\mathbf{r}, \mathbf{r}') dS' \right] \quad (25)$$

which may be differentiated again to yield

$$\frac{\partial^2}{\partial z^2} \phi(\mathbf{r}) = - \oint_C \mathbf{n} \bullet \hat{\mathbf{z}} s(\mathbf{r}') \frac{\partial}{\partial z} g(\mathbf{r}, \mathbf{r}') dl' - \lim_{\delta \to 0} \left[\int_{S-S_\delta} \frac{\partial \left(s(\mathbf{r}') - s(\mathbf{r}) \right)}{\partial z'} \frac{\partial g(\mathbf{r}, \mathbf{r}')}{\partial z'} dS' \right] \quad (26)$$

where we have used

$$\frac{\partial \left(s(\mathbf{r}') - s(\mathbf{r}) \right)}{\partial z'} = \frac{\partial s(\mathbf{r}')}{\partial z'}. \quad (27)$$

Using the two-dimensional divergence theorem, the second integral of (26) may be rewritten as

$$\int_{S-S_\delta} \frac{\partial \left(s(\mathbf{r}') - s(\mathbf{r}) \right)}{\partial z'} \frac{\partial g(\mathbf{r}, \mathbf{r}')}{\partial z'} dS' = - \int_{S-S_\delta} \left(s(\mathbf{r}') - s(\mathbf{r}) \right) \times \frac{\partial^2 g(\mathbf{r}, \mathbf{r}')}{\partial z'^2} dS' + \oint_{C+C_\delta} \mathbf{n} \bullet \hat{\mathbf{z}} \frac{\partial g(\mathbf{r}, \mathbf{r}')}{\partial z'} \left(s(\mathbf{r}') - s(\mathbf{r}) \right) dl. \quad (28)$$

As with (24), it can be shown that

$$\oint_{C_\delta} \mathbf{n} \bullet \hat{\mathbf{z}} \left(s(\mathbf{r}') - s(\mathbf{r}) \right) \frac{\partial g(\mathbf{r}, \mathbf{r}')}{\partial z'} dl = 0 \quad (29)$$

so that we have

$$\frac{\partial^2}{\partial z^2} \phi(\mathbf{r}) = -s(\mathbf{r}) \oint_C \mathbf{n} \bullet \hat{\mathbf{z}} \frac{\partial g(\mathbf{r}, \mathbf{r}')}{\partial z} dl + \lim_{\delta \to 0} \int_{S-S_\delta} \left(s(\mathbf{r}') - s(\mathbf{r}) \right) \frac{\partial^2 g(\mathbf{r}, \mathbf{r}')}{\partial z^2} dS' \quad (30)$$

the desired expression. Note that the source density should be Hölder-continuous [27] in order to pass a derivative through the surface integral. This is not an issue, since we will expand the current into functions that are differentiable in the region of the singularity. This holds even for pulse functions, since a pulse function will be centered on the singularity, and over the singularity the pulse function will be constant.

ACKNOWLEDGMENT

The authors would like to thank D. Gomez, UWM Electrical Engineering, for help with this project and R. Ancel, UWM Department of Mathematics, for helpful discussions concerning the two-dimensional divergence theorem.

REFERENCES

[1] T. Wu, "Introduction to Linear Antennas," in *Antenna Theory*, , Ed., R. E. Collin and F. J. Zucker, Eds. New York: McGraw-Hill, 1969, ch. 8, pt. 1.
[2] W. L. Stutzman and G. A. Thiele, *Antenna Theory and Design*. New York: Wiley, 1981.
[3] C. Balanis, *Advanced Engineering Electromagnetics*. New York: Wiley, 1989.
[4] R. Elliott, *Antenna Theory & Design*. New York: Wiley, 1981.
[5] *"NEC Manual"* [Online]. Available: http://www.nec2.org/
[6] S. Schelkunoff, *Advanced Antenna Theory*. New York: Wiley, 1952.
[7] B. Rynne, "On the well-posedness of Pocklington's equation for a straight wire antenna and convergence of numerical solutions," *J. Electromagn. Waves Applicat.*, vol. 14, pp. 1489–1503, 2000.
[8] G. Fikioris and T. T. Wu, "On the application of numerical methods to Hallen's equation," *IEEE Trans. Antennas Propag.*, vol. 49, no. 3, pp. 383–392, 2001.
[9] G. Fikioris, J. Lionas, and C. G. Lioutas, "The use of the frill generator in thin-wire integral equations," *IEEE Trans. Antennas Propag.*, vol. 51, no. 8, pp. 1847–1854, 2003.
[10] D. S. Jones, "Note on the integral equation for a straight wire antenna," *IEE Proc. Part H: Microw. Opt. Antennas*, vol. 128, no. 2, pp. 114–116, 1981.
[11] B. Rynne, "The well-posedness of the integral equations for thin wire antennas," *IMA J. Appl. Math.*, vol. 49, pp. 35–44, 1992.
[12] B. Rynne, "The well-posedness of the integral equations for thin wire antennas with distributional incidental fields," *Q. J. Mechanics Appl. Math.*, vol. 52, pp. 489–497, 1999.
[13] G. Fikioris and A. Michalopoulou, "On the use of entire-domain basis functions in Galerkin methods applied to certain integral equations for wire antennas with the approximate kernel," *IEEE Trans. Electromag. Compat.*, vol. 51, pp. 409–412, 2009.
[14] M. Silberstein, "Application of a generalized Leibnitz rule for calculating electromagnetic fields within continuous source regions," *Radio Sci.*, vol. 26, pp. 183–190, 1991.
[15] W.-X. Wang, "The exact kernel for cylindrical antenna," *IEEE Trans. Antennas Propag.*, vol. 39, no. 4, pp. 434–435, 1991.
[16] P. J. Davies, D. B. Duncan, and S. A. Funken, "Accurate and efficient algorithms for frequency domain scattering from a thin wire," *J. Comput. Phys.*, vol. 168, no. 1, pp. 155–183, 2001.
[17] D. H. Werner, J. A. Huffman, and P. L. Werner, "Techniques for evaluating the uniform current vector potential at the isolated singularity of the cylindrical wire kernel," *IEEE Trans. Antennas Propag.*, vol. 42, no. 11, pp. 1549–1553, 1994.
[18] D. H. Werner, "An exact formulation for the vector potential of a cylindrical antenna with uniformly distributed current and arbitrary radius," *IEEE Trans. Antennas Propag.*, vol. 41, no. 8, pp. 1009–1018, 1993.

[19] D. H. Werner, P. L. Werner, and J. K. Breakall, "Some computational aspects of pocklington's electric field integral equation for thin wires," *IEEE Trans. Antennas Propag.*, vol. 42, no. 4, pp. 561–563, 1994.
[20] O. P. Bruno and M. C. Haslam, "Regularity theory and superalgebraic solvers for wire antenna problems," *SIAM J. Sci. Comput.*, vol. 29, no. 4, pp. 1375–1402, 2007.
[21] A. Mohan and D. S. Weile, "Convergence properties of higher order modeling of the cylindrical wire kernel," *IEEE Trans. Antennas Propag.*, vol. 55, no. 5, pp. 1318–1324, 2007.
[22] A. Yaghjian, "Electric dyadic Green's functions in the source region," *IEEE Proc.*, vol. 68, pp. 248–263, 1980.
[23] A. Ishimaru, *Electromagnetic Wave Propagation, Radiation, and Scattering*. Englewood Cliffs, NJ: Prentice-Hall, 1991.
[24] G. W. Hanson and A. B. Yakovlev, *Operator Theory for Electromagnetics*. Berlin: Springer, 2001.
[25] R. Courant and D. Hilbert, *Methods of Mathematical Physics, Vol. II*. New York: Interscience, 1953.
[26] J. V. Bladel, *Electromagnetic Fields*, 2nd ed. Piscataway, NJ: Wiley-IEEE Press, 2007.
[27] O. D. Kellogg, *Foundations of Potential Theory*. Berlin: Springer Verlag, 1929.

Accelerated Source-Sweep Analysis Using a Reduced-Order Model Approach

Patrick Bradley, Conor Brennan, Marissa Condon, and Marie Mullen

***Abstract*—This communication is concerned with the development of a model-order reduction (MOR) approach for the acceleration of a source-sweep analysis using the volume electric field integral equation (EFIE) formulation. In particular, we address the prohibitive computational burden associated with the repeated solution of the two-dimensional electromagnetic wave scattering problem for source-sweep analysis. The method described within is a variant of the Krylov subspace approach to MOR, that captures at an early stage of the iteration the essential features of the original system. As such these approaches are capable of creating very accurate low-order models. Numerical examples are provided that demonstrate the speed-up achieved by utilizing these MOR approaches when compared against a method of moments (MoM) solution accelerated by use of the fast Fourier transform (FFT).**

***Index Terms*—Electromagnetic propagation, method of moments, projection algorithms.**

I. Introduction

The solution of electromagnetic wave scattering problems, from inhomogeneous bodies of arbitrary shape, is of fundamental importance in numerous fields such as geoscience exploration [1] and medical imaging [2]. For such problems, it is common to require the repeated solution of the electromagnetic wave scattering problem for a variety of source locations and types. This is of particular importance in the reconstruction of unknown material parameters in inverse problems and as such is a critical step in the optimization process [3].

Manuscript received November 26, 2010; revised January 24, 2011; accepted April 04, 2011. Date of publication August 12, 2011; date of current version November 02, 2011.

The authors are with the RF Modelling and Simulation Group, The RINCE Institute, School of Electronic Engineering, Dublin City University, Ireland (e-mail: bradleyp@eeng.dcu.ie; brennanc@eeng.dcu.ie).

Digital Object Identifier 10.1109/TAP.2011.2164210

Typically, the relevant integral equation (IE) is discretized using the MoM and results in a series of dense linear equations. The computational burden associated with the repeated solution of the full-wave scattering problem at each source location is severe, especially for large scatterers. Different strategies are used to accelerate the solutions of these linear systems. Considerable progress has been made in incorporating sparsification or acceleration techniques [4] and preconditioners into iterative methods which permit expedited solutions of the scattering problem. The CG-FFT solution in particular is often applied in situations where the unknowns are arranged on a regular grid.

An alternative approach is to develop approximate solutions to expedite the solution of EM scattering problems. Several approximations of the integral equation formulation are discussed in literature, including the Born approximations [5] and the family of Krylov subspace model order reduction techniques [6]. Although the Born approximation has been shown to efficiently simulate the EM response of dielectric bodies, these techniques are restricted to problems of relatively low frequencies and low contrast [5].

Krylov subspace approaches such as the Arnoldi algorithm [7]–[11] can produce very accurate low-order models since the essential features of the original system are captured at an early stage of the iteration. A set of vectors that span the Krylov subspace are used to construct the reduced order matrix model. By imposing an orthogonality relation among the vectors, linear independence can be maintained[1] and so high-order approximations can be constructed.

In this work, we modify the Arnoldi MOR procedure, introduced in [7], to efficiently perform scattering computations over a wide range of source locations for objects of varying inhomogeneity. We consider a two-dimensional dielectric object characterized by permittivity $\epsilon(\mathbf{r})$ and permeability μ for a TM^z configuration. A time dependence of $\exp(j\omega t)$ is assumed and suppressed in what follows. The corresponding integral equation can be expressed in terms of the unknown scattered field $E_z^s(\mathbf{r})$ and total field $E_z(\mathbf{r})$ [13]

$$E_z^s(\mathbf{r}) = \frac{j}{4}\int_V H_0^{(2)}\left(k_b|\mathbf{r}-\mathbf{r}'|\right) O(\mathbf{r}')E_z(\mathbf{r}')dv' \tag{1}$$

where $O(\mathbf{r}')$ is the object function at point $\mathbf{r}'$ given by

$$O(\mathbf{r}') = k^2(\mathbf{r}') - k_b^2. \tag{2}$$

The background wave number is given by k_b while $k(\mathbf{r}')$ is the wave number at a point in the scatterer. $H_0^{(2)}$ is the zero order Hankel function of the second kind. Using m pulse basis functions and Dirac-Delta testing functions [13], (1) is discretized by employing the MoM,[2] which results in the following matrix equation

$$(\mathbf{I} + \mathbf{GA})\mathbf{x} = \mathbf{b} \tag{3}$$

where $\mathbf{b}$ is the incident field vector at the center of each basis domain, $\mathbf{I}$ is an $m \times m$ identity matrix and $\mathbf{G}$ is an $m \times m$ matrix containing coupling information between the basis functions. $\mathbf{A}$ is an $m \times m$

[1]Note that due to finite precision computation loss of orthogonality between the computed vectors can occur in practical applications [6], [8], [12].

[2]Note that other basis and testing functions are possible without affecting the applicability of what follows.